

## Effect of *Anadara Granosa* Shell Volume Fraction on Erosive Wear and Hardness Behaviour of Al 6061 Metal Matrix Composites

Riki Hendra Purba<sup>1\*</sup>, Aldi Raditya Adriansyah<sup>2</sup>, James Julian<sup>3</sup>, Fitri Wahyuni<sup>4</sup>, Elvi Armadani<sup>5</sup>,  
Fathin Muhammad Mahdhudhu<sup>6</sup>

\*Email corresponding author: rikihendrapurba@upnvj.ac.id

Mechanical Engineering Department, Universitas Pembangunan Nasional Veteran Jakarta

Article history: Received: 22 November 2025 | Revised: 23 Desember 2025 | Accepted: 6 Januari 2026

**Abstract.** *Despite the favorable mechanical properties of Anadara Granosa Shell (AGS), particularly hardness, its influence on the wear resistance of Metal Matrix Composites (MMCs) remains insufficiently explored. Therefore, this study aims to investigate the potential of AGS waste as an eco-friendly reinforcement for Al6061 alloy. Composites were fabricated with 0 wt%, 5 wt%, 10 wt%, and 15 wt% AGS addition. Wear behavior of each specimen was evaluated using sandblast with SiO<sub>2</sub> as the erodent particles. The investigation also involved the microstructure and wear mechanism observation using optical microscope and Scanning Electron Microscopy (SEM). In addition, the hardness of each material measurement using Vickers hardness test was included to obtain a comprehensive insight. The results shows that the AGS reinforcement was evenly distributed within the matrix, though a minor presence of voids was observed. The hardness of specimens exhibited a consistent increase proportional to the AGS content. Interestingly, the erosion rate showed no significant difference between the 0 wt% and 5 wt% AGS additions, but drastically increased with 10 wt% and 15 wt% reinforcement. This suggests that hardness is not the primary factor governing the erosion behavior in these composites. Analysis of the worn surfaces revealed a prevalent wear mechanism: reinforcement particle peel-out, which became more severe at 10 wt% and 15 wt% AGS concentrations. Conversely, the unreinforced (0 wt%) Al 6061 alloy displayed ripple formation, indicating a plastic deformation mechanism typical of a ductile material. Therefore, this study highlights the critical importance of considering the wear mechanism, specifically the susceptibility to particle pull-out, when evaluating the erosive wear behavior of Al6061 MMCs reinforced with Anadara Granosa Shell waste.*

**Keywords** - Al 6061, *Anadara granosa*, Metal Matrix Composites (MMC), Erosive Wear, Vickers Hardness

### INTRODUCTION

Waste management presents a major global environmental challenge, particularly in Indonesia. The significant and rising volume of shells from blood cockle (*Anadara granosa*), a popular high-protein food source, has created a substantial domestic waste issue. For instance, national production reached 373,202 tons in 2011, subsequently generating massive quantities of underutilized waste. Local estimates, such as those in Sukoharjo in 2019, indicated a daily disposal rate of 360 kg of this shell waste [1]. This growing problem necessitates the development of alternative, value-added solutions to mitigate waste volume.

Composite materials, defined as the combination of two or more distinct phases, often exhibit superior properties compared to their individual constituents [2]. Typically consisting of a matrix and a reinforcement, these materials are widely employed in advanced engineering applications. The Al6061 alloy is a preferred Aluminum Matrix Composite (AMC) for technical sectors, including transportation and construction, owing to its outstanding mechanical characteristics, such as high tensile strength and favorable hardness. This alloy offers an ideal balance of strength, durability, and processing ease [3], [4]. Nevertheless, the deployment of these materials in demanding environments is frequently limited by degradation phenomena, especially erosive wear.

Erosive wear is a critical problem in high-stress industrial settings, characterized by the volume of material loss resulting from the impingement of high-velocity particles on a surface. The key influencing factors include impact dynamics (e.g., particle velocity and angle), material failure mechanisms (e.g., deformation, cutting, and cracking), and inherent material properties (e.g., hardness, toughness, ductility, and brittleness) [5], [6]. Erosive damage is a major concern that affects heavy machinery and components operating under extreme conditions, such as gas and aircraft engines, industrial piping systems, and components in the mining industry [7]–[14]. Consequently, further investigation is essential to identify factors that can reduce the severity of wear [15].

Addressing these challenges presents an opportunity to utilize Al6061 and AGS waste for composite production. Previous studies have established the potential of shell powder as a natural, eco-friendly reinforcement. Research by Suleiman [16] demonstrated that adding shell powder (from 0 wt% to 15 wt%) significantly enhanced the tensile and flexural strength of aluminum composites, with the highest flexural strength of 165.51 MPa achieved at 15 wt%.

Similarly, Nayan and Hafli [17] found high peak tensile strengths (107.45 MPa and 107.60 MPa for 20% and 40% volume fractions, respectively) in shell particle composites. The shell's composition, rich in calcium oxide (66.70%) and magnesium oxide (22.28%), endows it with excellent mechanical properties suitable for improving the strength-to-weight ratio of composite applications. However, the existing literature exhibits significant gaps.

Prior research has focused predominantly on the static mechanical properties (tensile and flexural strength) of Anadara granosa shell powder, primarily in polymer matrices (e.g., polyester resin) [16], [17]. A critical oversight is the neglect of the dynamic performance characteristic of erosive wear resistance, which is vital for demanding industrial applications (such as in aerospace and transportation). Furthermore, the transition of this natural reinforcement into a high-performance Aluminum Matrix Composite (AMC), specifically with the widely used Al 6061 alloy, and the optimization of its volume fraction for wear mitigation have yet to be thoroughly investigated. Therefore, this study aims to fill this knowledge gap by comprehensively analyzing the erosive wear mechanism of Al 6061 composites reinforced with varied weight fractions (0 wt%, 5 wt%, 10 wt%, and 15 wt%) of Anadara granosa shells. The performance is specifically evaluated under a sand blasting process, which simulates the real-world erosive conditions critical for high-performance material systems.

## METHODS

### Specimen Manufacturing and Preparation

The base material chosen for the composite matrix was the commercial Al6061 alloy, which is highly favored in engineering applications, particularly in the transportation and construction sectors, owing to its superior combination of good mechanical properties and high corrosion resistance. Al 6061 is characterized by a low density, approximately 2.7 kg/m<sup>3</sup>, which is about one-third the density of steel, making it ideal for applications requiring light yet strong materials such as aircraft structures and transportation equipment. The alloy demonstrates a tensile strength of around 134.8 MPa and a Brinell hardness (BHN) of 62.8 [4]. This material was utilized in plate form to facilitate the casting process. The Vanta Family X-Ray Fluorescence Analyzer is used to see the chemical composition of the alloy, the results are shown in Table 1.

**Table 1.** Chemical composition of Al6061 [4]

Element	Fe	Si	Cu	Mn	V	Ti	Al
<b>Standard Weight %</b>	0.17	0.63	0.32	0.52	0.01	0.02	Bal.
<b>Tested Weight %</b>	0.31	0.63	0.18	0.03	0.01	0.43	Bal.

The reinforcement material utilized was the Anadara granosa shell, which presents an eco-friendly solution for composite enhancement due to its chemical composition. The high content of calcium oxide (CaO) and magnesium oxide (MgO) within the shells contributes favorably to the mechanical properties, including tensile strength, and is ideal for increasing the strength-to-weight ratio of composite materials. The shells naturally possess a hard yet light nature. Previous research has confirmed the effectiveness of this powder as a natural reinforcement, showing significant increases in tensile strength and flexural strength up to 107.60 MPa at a certain volume fraction. The material parameters are shown in Table 2 [17]. The reinforcement material was prepared in powder form and incorporated into the aluminum matrix in varying volume fractions: 0 wt%, 5 wt%, 10 wt%, and 15 wt%. The volume fraction can be calculated using the following formula:

$$V_f = V_{fiber}\% \times V_{mold} \quad (1)$$

**Table 2.** Chemical Composition Andara Granosa [17]

Chemical Components	Composition
<b>CaO</b>	66.70
<b>SiO<sub>2</sub></b>	7.88
<b>Fe<sub>2</sub>O<sub>3</sub></b>	0.03
<b>MgO</b>	22.28
<b>Al<sub>2</sub>O<sub>3</sub></b>	1.25

The specimens were fabricated using the sand casting method. First, the Al6061 alloy matrix was melted in a furnace/kiln at approximately 700°C. The predetermined amounts of AGS powder were incorporated as reinforcement into the sand molds. The four distinct volume fractions (Vf) of the AGS powder were investigated. After that, the reinforcement AGS was poured into the furnace and manually stirred to ensure the homogenizing distribution of AGS in molten Al6061. Then, the molten was subsequently poured into prepared sand molds with dimension 55 mm x 55 mm x 15 mm, as shown in Figure 2. Finally, the molten was cooled at room temperature with approximately three hours as cooling time. Following complete solidification, the cast composites were extracted and machined to the final testing dimensions. A total of 12 specimens, each with the same dimensions, measuring 50mm x 50mm x 10mm, were prepared for analysis. Before the testing, all specimen surfaces underwent meticulous preparation, which involved systematic grinding with progressively finer sandpaper grits, culminating in a final polishing step to achieve a smooth, mirror-like finish crucial for accurate testing.

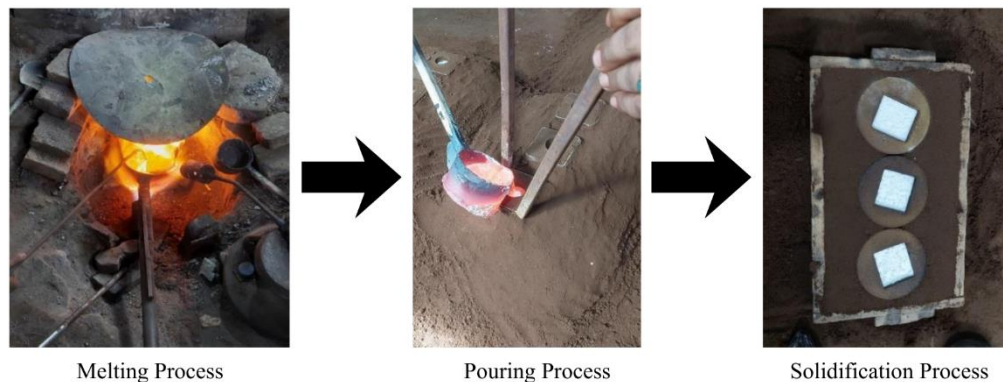


**Figure 1.** Specimen Fabrication

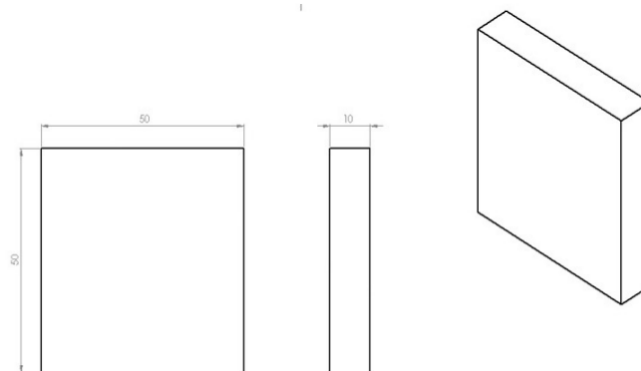


**Figure 2.** Specimen Geometry

### Vickers Hardness Test

Vickers hardness tester Vf-300 has been used as a Vickers hardness machine. Before the Vickers hardness test was carried out, every targeted material was cut with the dimensions mentioned before, and polished. The procedure began with the precise positioning of the prepared specimen on the test stage. An indenter, a diamond pyramid with an angle of 136° between opposite faces, was pressed onto the specimen surface under a specific load (F) for a duration of 10 to 15 seconds to ensure optimal indentation. After removing the load, the resulting diamond-shaped indentation marks were observed and measured using a microscope attached to the apparatus to determine the diagonal lengths (d1 and d2). To ensure accurate data and to assess the uniformity of hardness across the composite, the test was performed with 14 repetitions at different locations on each specimen.

### Erosion Resistance Test

Erosion resistance was evaluated using the sand blasting method (as schematically shown in Figure 4), a technique designed to simulate and quantify material degradation caused by the high-velocity impact of abrasive particles. The procedure began with cleaning and accurately weighing each specimen using a balance. The abrasive medium used was silica sand (SiO<sub>2</sub>), stored in a shot hopper. Key testing parameters were rigorously controlled: the air pressure was adjusted via a compressor and pressure gauge to maintain a nozzle pressure of 0.49 MPa, and the test was performed at a fixed impact angle ( $\alpha$ ) of 30°. This 30° angle was specifically chosen as it is the expected angle for

maximum erosion on ductile materials like aluminum [18]. The abrasive particles were accelerated through a nozzle and impacted the specimen surface, with the total duration of the exposure set to 10 minutes.

Before and after the test, the mass of each specimen was weighed by an electronic scale then the volumetric loss was calculated. The volumetric loss was divided by the total feed erodent to find the erosion rate. The erosion scar of the worn surface and the vertical section of the erodent surface were examined to determine the possible erosion mechanism.

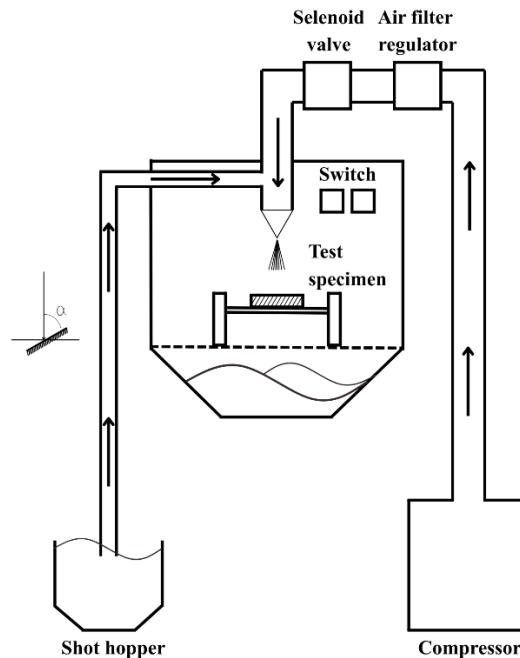


Figure 3. Schematic View Sand Blasting

### Microstructural and Wear Mechanism Analysis

The microstructural observations were conducted using both an Optical Microscope and a Scanning Electron Microscope (SEM). The Optical Microscope was primarily used to examine the specimens after the polishing and etching processes, to identify phase changes, particle dispersion, and the presence of gross defects, such as voids and agglomeration within the Al6061 matrix. The effectiveness of particle incorporation and bonding was initially assessed at this stage. The Scanning Electron Microscope (SEM) provided high-resolution images to confirm the morphology of the reinforcement particles, detail the matrix-reinforcement interfacial bonding, and accurately identify microscopic defects such as micro-cracks, porosity, and particle pull-out phenomena, which significantly influence mechanical performance. Crucially, the SEM was also used for the post-erosion analysis to study the wear mechanism on the surface of the sand-blasted specimens. This included observing features like plastic deformation ripples and peel-out, providing insights into how the composite failed under abrasive impact.

## RESULT AND DISCUSSION

### Microstructure and Optical Analysis

Initial visual and microstructural analysis, as illustrated in Figure 5, revealed significant findings regarding the incorporation of the AGS powder into the Al6061 matrix. Macroscopic observation indicated that while the pure Al6061 (0% Vf) exhibited minimal porosity, increasing the reinforcement volume fraction led to a sharp rise in defects, notably including porosity and particle agglomeration. The initial preparation phase confirmed the presence of the reinforcement particles as a dark phase distributed within the bright aluminium matrix, but critically highlighted the occurrence of voids at the particle-matrix interface. These interfacial voids are primarily attributed to two mechanisms: poor wettability between the ceramic phase and the molten aluminium, and shrinkage during casting. Both factors collectively compromise the material's mechanical integrity. The general trend confirmed that higher volume fractions, particularly at 10 wt% and 15 wt%, result in reduced homogeneity and consequently increase the likelihood of both agglomeration and void formation.

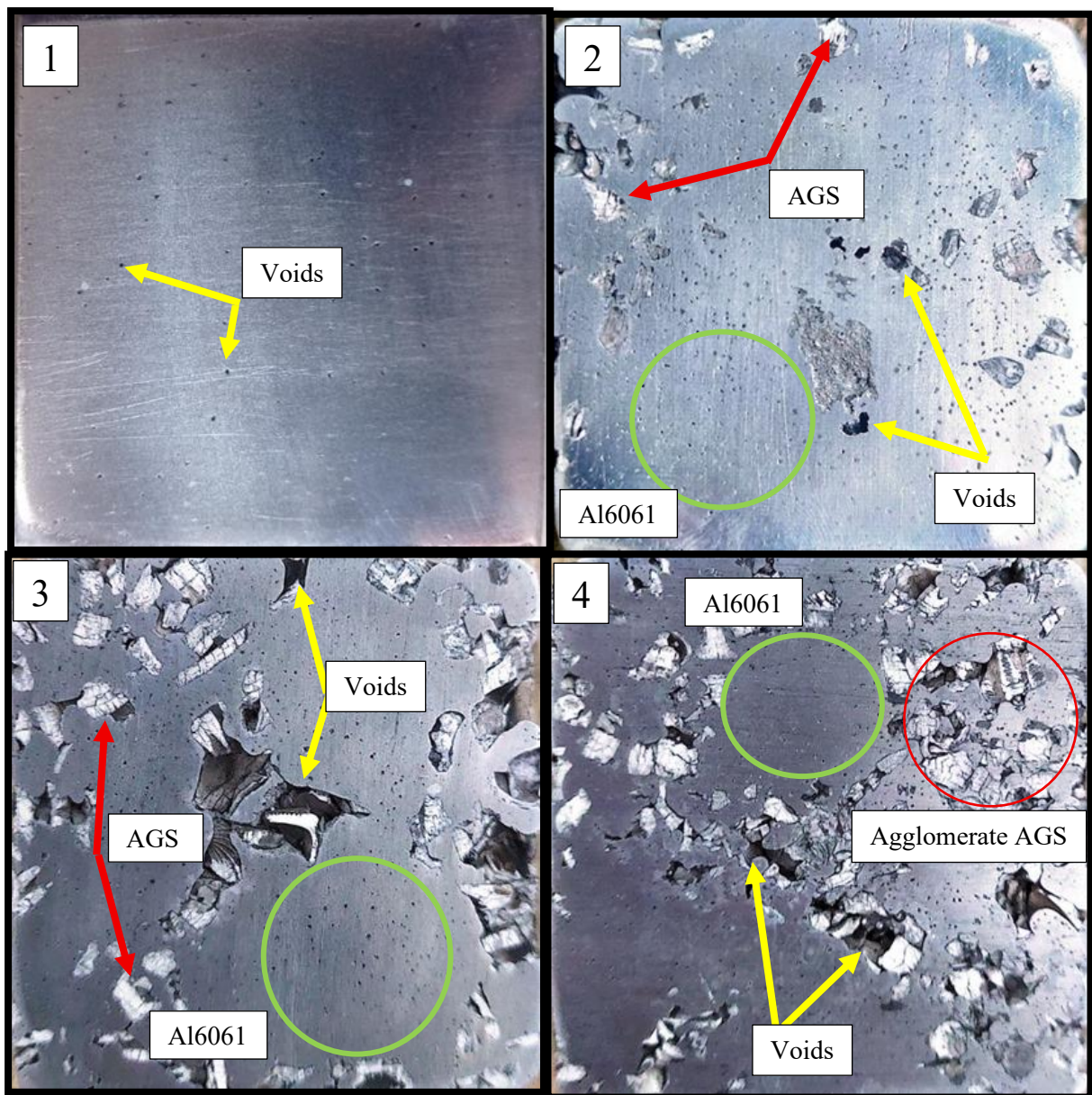


**Figure 4.** Visual Results of Al 6061 and Shell Composite

The high-resolution imaging from the Scanning Electron Microscope, as shown in Figure 6 and Figure 7, provided detailed confirmation of the two-phase nature and interface quality of the composite. At both x500 and x1000 magnifications, the matrix (darker grey) and the reinforcement particles (brighter phase) were clearly distinguishable. The SEM confirmed that while AGS particles could adhere well to the matrix in certain areas, it also clearly revealed microscopic voids and gaps along the phase boundaries. At higher volume fractions (15%), the increased particle clustering resulted in more extensive agglomeration, which is a structural defect that acts as a stress concentration point, potentially leading to premature crack initiation. The presence of these microstructural discontinuities, particularly the voids and poor bonding identified by the SEM, suggests a direct link to the predicted performance in hardness and erosion tests.

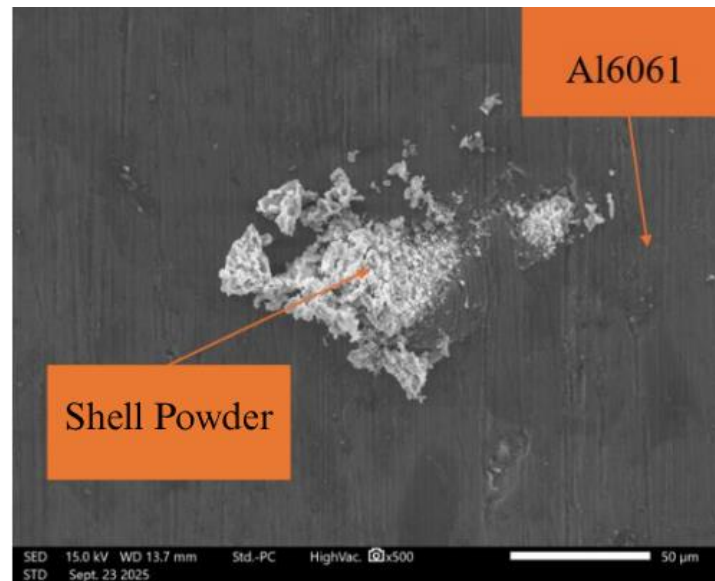


Figure 5. SEM test results with x500 magnification of Al 6061 composite and AGS

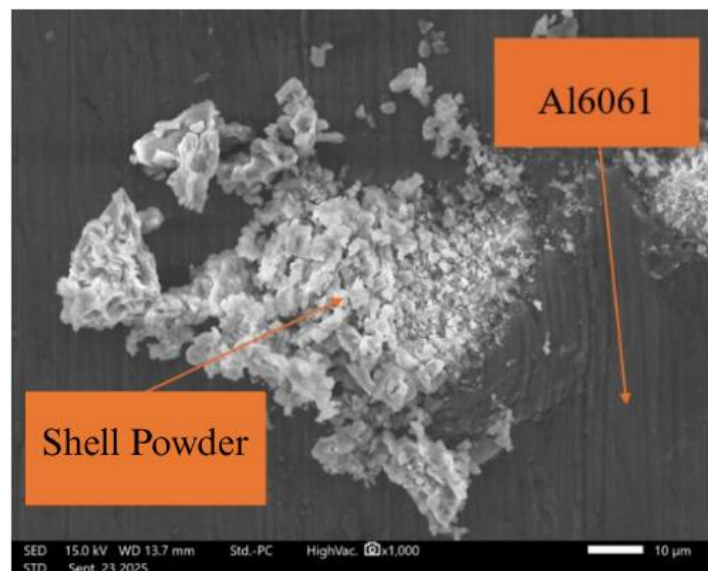


Figure 6. SEM test results with x1000 magnification of Al 6061 composite and AGS

### Vickers Hardness Test Results

Vickers Hardness testing demonstrated a consistent and proportional increase in hardness with respect to the volume fraction of the AGS reinforcement powder, as presented in Figure 8. A one-way ANOVA test, shown in Table 3, was conducted to see the changes in hardness with the increasing volume fractions. The pure Al6061 matrix (0% Vf) recorded an average hardness of  $31 \pm 2.7$  HV. This value substantially increased by approximately 29% to  $40 \pm 5.2$  HV at 5% Vf, confirming that the shell particles had begun to effectively reinforce the ductile aluminium matrix. This trend persisted, with the 10% Vf specimen achieving  $49 \pm 11.6$  HV, which represents an overall increase of approximately 57% compared to the pure matrix. The highest average hardness of 54 HV (a 75% increase) was recorded at the 15% Vf. This significant enhancement is primarily attributed to the presence of hard particles acting as effective barriers to dislocation movement within the matrix, consequently increasing the material's resistance to plastic deformation.

**Table 3.** One-way ANOVA test for Vickers hardness testing

Source of Variation	SS	df	MS	F	P-value	F crit
Between Groups	2213,401	2	1106,701	19,51958	1,34E-06	3,238096
Within Groups	2211,181	39	56,69696			
Total	4424,583	41				

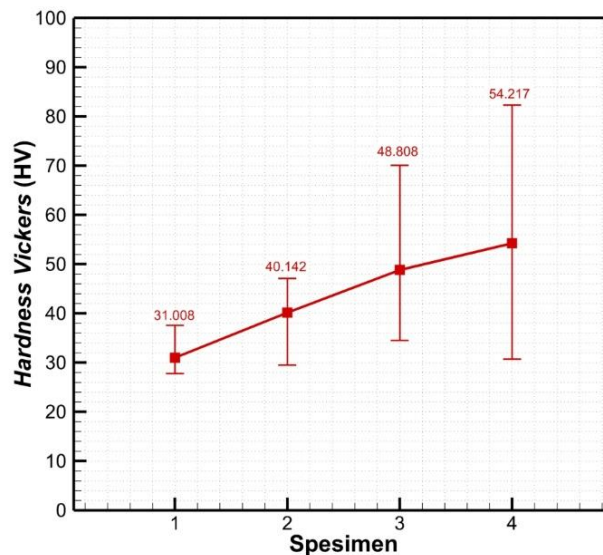


**Figure 7.** Vickers Hardness Results Graph of Each Volume Fraction

### Erosion Rate Results

The erosion testing was focused on an impact angle of 30°. A one-way ANOVA test was conducted after the erosion testing to see the effect of increasing the AGS volume fraction on the erosion rate of the MMC, the result is shown in Table 4. The erosion test results showed a trend of increasing erosion rate corresponding to the increase in the volume fraction (Vf) of the *Anadara granosa* reinforcement, as shown in Figure 9. The baseline pure Al6061 (Specimen No. 1) recorded an erosion rate of  $19.708 \pm 0.001 \times 10^{-2} \text{ cm}^3/\text{kg}$ . With the introduction of 5% Vf reinforcement (Specimen No. 2), the erosion rate slightly increased to  $20.870 \pm 0.02 \times 10^{-2} \text{ cm}^3/\text{kg}$ , representing an increase of 5.89%. However, A significant increase was observed at 10% Vf (Specimen No. 3), with the rate climbing to  $28.470 \pm 0.01 \times 10^{-2} \text{ cm}^3/\text{kg}$  (a 36.38% increase from Specimen No. 2). The highest erosion rate was recorded at 15% Vf (Specimen No. 4) at  $31.949 \pm 0.03 \times 10^{-2} \text{ cm}^3/\text{kg}$ .

Generally, increasing the volume fraction of Anadara granosa shells (AGS) can lead to an increase in the erosion rate, as demonstrated in the present study. Conversely, in a study by Lal et al. [19], the addition of shell particles improved sliding wear resistance in AA6061 composites, where the normal load was identified as the dominant factor, contributing 71.34% to the wear rate. However, Dwivedi et al. [20] states that while increasing the shell content initially reduced the coefficient of friction (CoF) due to enhanced hardness, further reinforcement beyond an optimal threshold caused the wear rate to increase. This latter observation aligns with the current study, where the erosion rate increased significantly above 10%Vf. This detrimental outcome is primarily attributed to the presence of microstructural defects, such as increased porosity and particle agglomeration, and poor matrix-reinforcement wettability which compromise the structural integrity of the composite and consequently accelerate material removal under erosive conditions.

**Table 4.** One-way ANOVA test for erosion testing

Source of Variation	SS	df	MS	F	P-value	F crit
Between Groups	0,024174	3	0,008058	11,5143	0,006684	4,757063
Within Groups	0,004199	6	0,0007			
Total	0,028373	9				

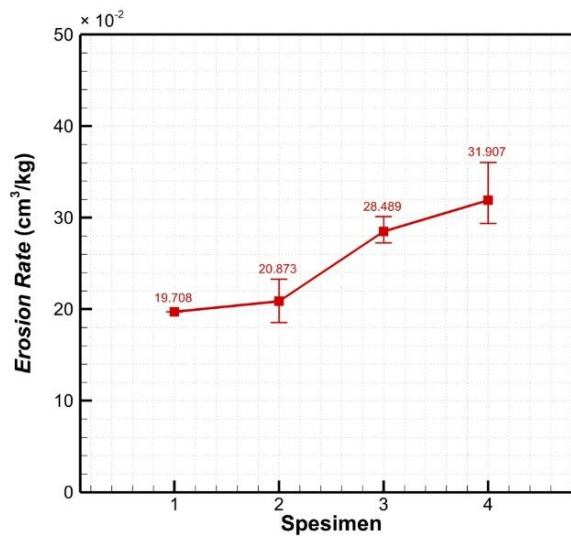


**Figure 8.** Erosion Rate Results Graph for Each Volume Fraction

#### Vickers Hardness vs Erosion Rate

The comparison between the Vickers hardness and erosion rate results in different volume fractions is illustrated in the combined graph shown in Figure 10. The data reveal a consistent upward trend in bulk hardness, peaking at 54 HV for the 15% volume fraction. However, this increase in hardness is accompanied by a rise in the erosion rate, particularly beyond the 5% threshold, where values climb from  $19.708 \times 10^{-2} \text{ cm}^3/\text{kg}$  to  $31.907 \times 10^{-2} \text{ cm}^3/\text{kg}$ . This phenomenon suggests that while the shell reinforcement enhances surface resistance to static indentation, the presence of casting defects such as porosity and particle agglomeration at higher concentrations promotes a shift in the wear mechanism from plastic deformation to brittle particle peel-out, ultimately reducing the composite's overall erosive resistance.

A study conducted by Sagar et al. [21], shows a similar tendency, that increasing the volume fractions of SiC and Fly ash consistently raises the hardness of the Al6061 matrix. Yet, wear resistance decreases drastically when the volume fraction increases beyond 5%, but increases again when the fly ash is at 7%. However, another study by Suresh et al. [22], shows that adding TiB<sub>2</sub>, improves the sliding wear resistance of Al6061. The hardness of the composite also increases with the increasing volume fraction of the TiB<sub>2</sub>. The primary factor driving these divergent results is the interfacial bonding quality and microstructural integrity of the composite. In the case of AGS, higher concentrations lead to poor wettability and shrinkage during casting, which creates interfacial voids and weakens the matrix-reinforcement bond. These structural discontinuities act as stress concentration points, causing hard particles to be easily detached or "peeled out" under high-velocity erosive impacts, unlike synthetic reinforcements, which may maintain better cohesion at higher loading levels.

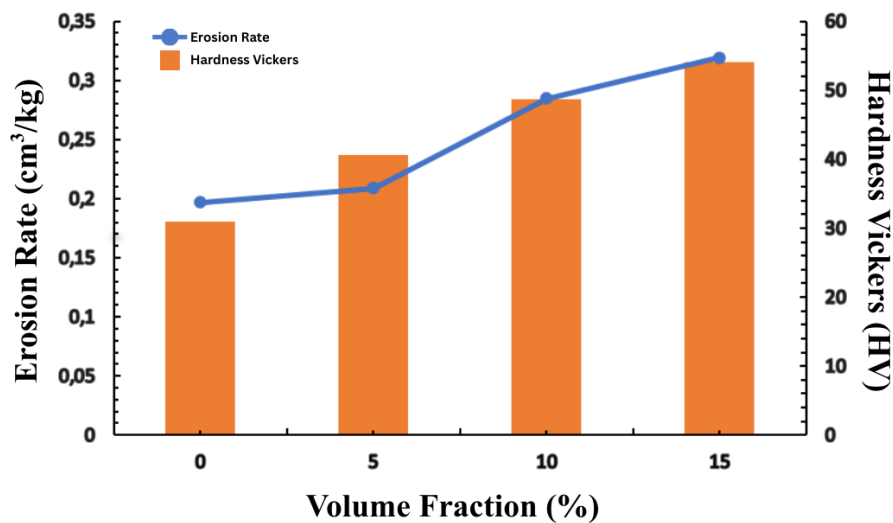


Figure 9. Vickers hardness vs Erosion rate graph

### Wear Mechanism Analysis

Analysis of the eroded specimen surfaces, as shown in Figure 11, confirmed that material degradation under sand blasting was governed by a combination of mechanisms, consistent with the composite's mixed ductile-brittle nature. Since the matrix (Al6061) is ductile, the surface exhibited clear patterns of plastic deformation, manifested as ripples (wave-like patterns) across all specimens, oriented transverse to the particle impact direction. The presence of these ripples is characteristic of ductile erosion mechanisms where the material deforms plastically rather than fracturing instantaneously.

However, the brittle nature of the *Anadara granosa* reinforcement introduced secondary, more destructive wear modes. In the pure Al 6061 specimen (No. 1), ripples were clear and peel-out (particle detachment) was minimal. As the volume fraction increased, the density of microstructural defects intensified. Specimens with 5% and 10% Vf (No. 2 and No. 3) showed increasing evidence of peel out and larger, more frequent voids. These voids and the weakened interfacial bonding facilitated the removal of entire reinforcement particles by the impact of the erodent, directly accelerating the rate of material loss.

The specimen with the highest volume fraction (No. 4) exhibited the most severe damage, dominated by large, widespread voids and extensive peel-out that masked the regular ripple pattern. The increased susceptibility to erosion at higher reinforcement fractions is therefore a consequence of a shift in the failure mechanism: the hard particles do increase bulk hardness, but the accompanying casting defects (poor interfacial bonding, porosity, and agglomeration) promote brittle failure via particle detachment, thereby overcoming the matrix's inherent ductility advantage and leading to a higher overall erosion rate.

Thus, the relationship between the particle size of AGS, porosity, and the resulting particle pull-out phenomenon is a fundamental factor governing the erosive wear characteristics of Al-6061 composites. While increasing the AGS volume fraction enhances the material's bulk hardness by creating barriers to dislocation movement, it simultaneously introduces structural defects such as porosity and interfacial voids due to poor wettability and casting shrinkage. At higher concentrations, particularly at 10 wt% and 15 wt%, these reinforcement particles tend to agglomerate, creating stress concentration points that weaken the interfacial bond between the matrix and the reinforcement. During sandblasting at a critical 30° impact angle, the high-velocity erodent particles exploit these weakened interfaces, causing a shift in the wear mechanism from ductile plastic deformation to brittle failure characterized by massive particle peel-out. Consequently, the detachment of these hard particles leaves behind significant craters on the surface, directly accelerating the volumetric erosion rate and explaining why higher reinforcement levels lead to reduced erosive resistance despite superior nominal hardness.

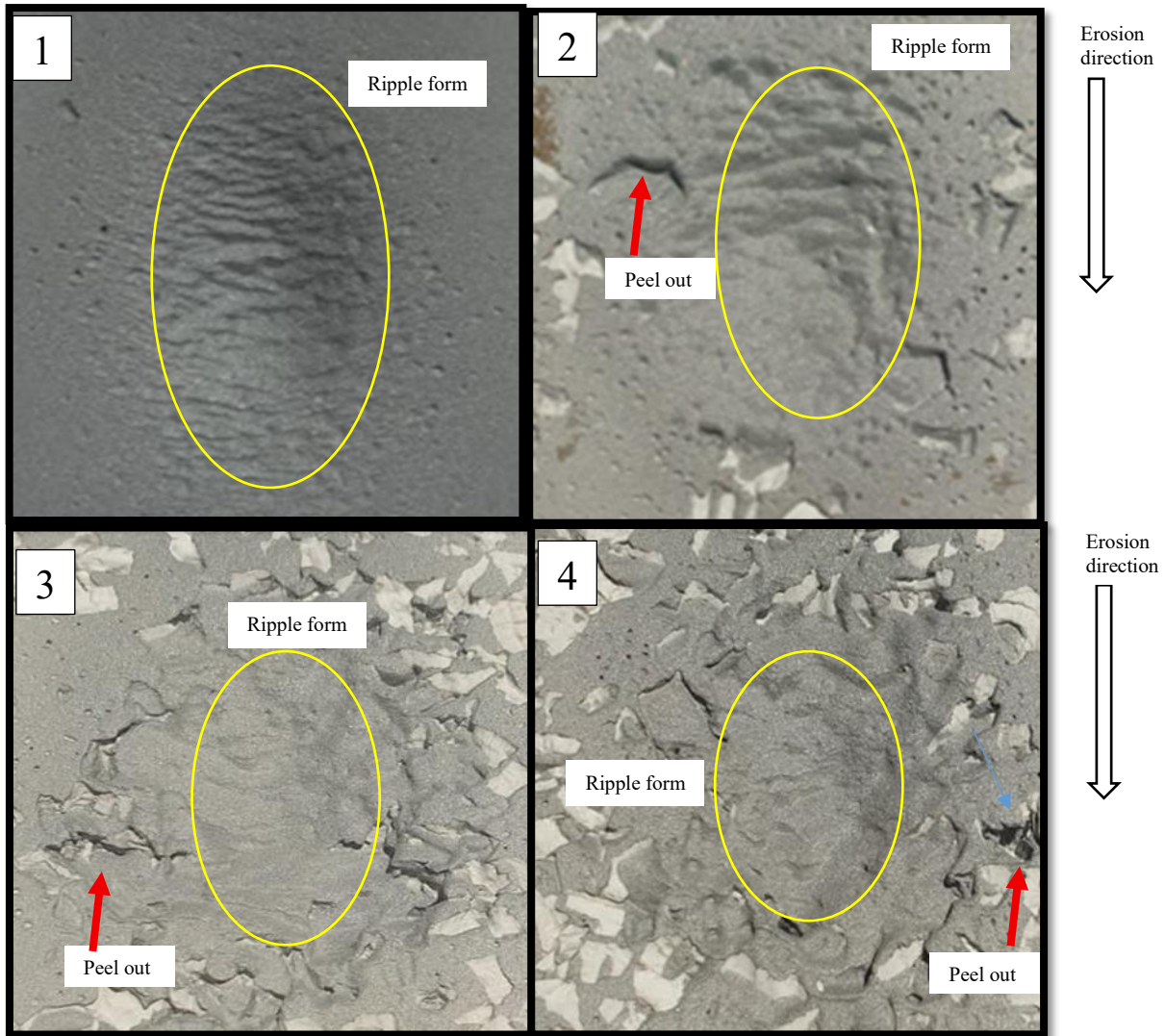


**Figure 10.** Observation of the surface of the specimen that has experienced erosion wear

## CONCLUSION

Based on the present research investigating the influence of varying volume fractions of Anadara granosa shell powder on the erosion resistance of Al6061 composites, the following conclusions are drawn:

1. The addition of AGS powder significantly influenced the material's mechanical properties. The hard  $\text{CaCO}_3$ -rich reinforcement acted as a barrier to dislocation movement, leading to a substantial increase in Vickers hardness across all composite variants compared to the pure Al 6061 matrix.
2. At lower volume fractions (e.g., 5%), the particles were relatively well-distributed, enhancing hardness without severely compromising ductility. However, at higher volume fractions (10% and 15%), microstructural analysis confirmed dominant particle agglomeration and increased void formation due to poor matrix-reinforcement wettability, resulting in reduced structural homogeneity and increasing the standard deviation of hardness values.
3. The erosion test, performed at the critical ductile angle of  $30^\circ$ , demonstrated that increasing the reinforcement fraction led to an overall increase in the volumetric erosion rate. This higher erosion rate, despite the increased bulk hardness, is directly attributed to the microstructural defects (voids and poor bonding) which promoted a shift in the wear mechanism towards brittle failure (peel-out of particles), accelerating mass loss.
4. Considering the balance between increased mechanical properties and resistance to material degradation, the optimal volume fraction of Anadara granosa powder for maximizing both mechanical stability and erosion performance in the Al6061 composite is approximately 5%, which yielded lower erosion susceptibility compared to higher fractions.

## REFERENCES

- [1] R. Andika and H. A. Safarizki, "Pemanfaatan limbah cangkang kerang dara (*Anadara granosa*) sebagai bahan tambah dan komplemen terhadap kuat tekan beton normal," *MoDuluS: Media Komunikasi Dunia Ilmu Sipil*, vol. 1, no. 1, pp. 1-6, 2019.
- [2] W. D. Callister and D. G. Rethwisch, *Materials science and engineering: An introduction*, 10th ed. Hoboken, NJ, USA: Wiley, 2018.
- [3] K. Dash, S. Sukumaran, and B. C. Ray, "The behaviour of aluminium matrix composites under thermal stresses," *Science and Engineering of Composite Materials*, vol. 23, no. 1, pp. 1-10, 2016.
- [4] T. V. Christy, N. Murugan, and S. Kumar, "A comparative study on the microstructures and mechanical properties of Al 6061 alloy and the MMC Al 6061/TiB<sub>2</sub>/12P," *Journal of Minerals & Materials Characterization & Engineering*, vol. 9, no. 1, 2010.
- [5] I. Finnie, "Erosion of surfaces by solid particles," *Wear*, vol. 3, no. 2, pp. 87-103, 1960.
- [6] T. Deng, "Erosive Wear Mechanisms of Materials—A Review of Understanding and Progresses," *Materials*, vol. 18, no. 7, p. 1615, 2025.
- [7] K. Shimizu, N. Uemura, H. Kido, J. Yamabe, and S. Sasaki, "Microstructural evaluation and high-temperature erosion characteristics of high chromium cast irons," *Wear*, vol. 426-427, no. Part A, pp. 420-427, 2019.
- [8] K. Kusumoto, N. Uemura, H. Kido, K. Shimomura, and J. Yamabe, "Effect of carbide refinement on high temperature erosive wear behavior of high chromium white cast iron with different titanium and carbon additions," *Materials Today Communications*, vol. 39, p. 109276, 2024.
- [9] A. Espinoza-Jara, M. Walczak, G. V. Messa, W. Brevis, A. Pascone, and C. Tedeschi, "Experimental insights into sweep-induced mechanism of erosive wear in a straight pipe section with turbulent slurry flow," *Wear*, vol. 580-581, p. 206221, 2025.
- [10] Itz, "Erosion in nuclear piping systems," *Journal of Pressure Vessel Technology*, vol. 132, no. 2, p. 024501, 2010.
- [11] K. Amagata, T. Hayashi, and T. Takano, "Experiments on liquid droplet impingement erosion by high-speed spray," *Nuclear Engineering and Design*, vol. 250, pp. 101-107, 2012.
- [12] P. L. Johansen, S. Bernad Jr., and S. Kiil, "Rain erosion of wind turbine blade coatings using discrete water jets: Effects of water cushioning, substrate geometry, impact distance, and coating properties," *Wear*, vol. 328-329, pp. 140-148, 2015.
- [13] B. S. Mann and V. Arya, "HVOF coating and surface treatment for enhancing droplet erosion resistance of steam turbine blades," *Wear*, vol. 254, no. 6, pp. 652-667, 2003.
- [14] M. Ahmad, M. Schatz, and M. V. Casey, "An empirical approach to predict droplet impact erosion in low-pressure stages of steam turbines," *Wear*, vol. 402-403, pp. 57-63, 2018.
- [15] P. Stodola, Z. Jamrichova, and J. Stodola, "Modelling of erosion effects on coatings of military vehicle components," *TRANSACTIONS of FAMENA*, vol. 36, no. 3, pp. 33-38, 2012.
- [16] I. Y. Suleiman, A. Kasim, A. T. Mohammed, and M. Z. Sirajo, "Evaluation of mechanical, microstructures and wear behaviours of aluminium alloy reinforced with mussel shell powder for automobile applications," *Strojniški vestnik – Journal of Mechanical Engineering*, vol. 67, no. 1-2, pp. 27-35, 2021, doi: 10.5545/sv-jme.2020.6953.
- [17] A. Nayan and T. Hafli, "Analisa struktur mikro material komposit polimer berpenguat serbuk cangkang kerang," *Malikussaleh Journal of Mechanical Science and Technology*, vol. 6, no. 1, pp. 15-24, 2022.
- [18] I. Finnie, "Some observations on the erosion of ductile metals," *Wear*, vol. 19, pp. 81-90, 1972.
- [19] C. Lal, S. Tejyan, and V. Singh, "Fabrication and Sliding Wear Characterization of Eggshell Particulate Reinforced AA6061 Alloy Metal Matrix Composites," *Tribology in Industry*, vol. 46, no. 1, pp. 29-38, 2024.
- [20] S. K. Dwiwedi, A. K. Srivastava, and M. Chopkar, "Fabrication and dry sliding wear study of Al6061/mussel-shell particulate composites," *SN Applied Sciences*, vol. 1, no. 721, pp. 1-13, Jun. 2019.
- [21] S. K. Murmu et al., "Exploring tribological properties in the design and manufacturing of metal matrix composites: an investigation into the AL6061-SiC-fly ASH alloy fabricated via stir casting process," *Front. Mater.*, vol. 11, Art. no. 1415907, May 2024.
- [22] S. Suresha, N. S. V. Moorthi, dan C. E. Prema, "Tribological and Mechanical behavior study of Al6061-TiB<sub>2</sub> Metal Matrix Composites using Stir Casting," *Advanced Materials Research*, vol. 984-985, hlm. 200-206, Juli 2014.

(This page is intentionally left blank)